processes

MDPI

Article

Structure Property Investigation of Glass-Carbon Prepreg Waste-Polymer Hybrid Composites Degradation in Water Condition

Norlin Nosbi [1,*], Haslan Fadli Ahmad Marzuki [2], Muhammad Razlan Zakaria [3], Wan Fahmin Faiz Wan Ali [4], Fatima Javed [5] and Muhammad Ibrar [6]

1 Department of Mechanical Engineering, Centre for Corrosion Research (CCR), Institute of Contaminant Management for Oil and Gas, Universiti Teknologi PETRONAS, Seri Iskandar 32610, Perak, Malaysia
2 SIRIM Kulim, Kulim Hi-Tech Park, Kulim 09000, Kedah, Malaysia; haslan@sirim.my
3 Faculty of Chemical Engineering Technology, Universiti Malaysia Perlis (UniMAP), Perlis, Malaysia; razlan.usm@gmail.com
4 School of Mechanical Engineering, Faculty of Engineering, Universiti Teknologi Malaysia, Skudai 81310, Johor, Malaysia; wan_fahmin@utm.my
5 Department of Chemistry, Shaheed Benazir Bhutto Women University, Peshawar 25000, Khyber Pakhtunkhwa, Pakistan; fatimajaved@ymail.com
6 Department of Physics, Islamia College University, Peshawar 25000, Pakistan; ibrar@icp.edu.pk
* Correspondence: norlin.nosbi@utp.edu.my; Tel.: +605-368-7145

Received: 16 May 2020; Accepted: 11 September 2020; Published: 10 November 2020

Abstract: The limited shelf life of carbon prepreg waste (CPW) from component manufacturing restricts its use as a composite reinforcement fibre on its own. However, CPW can be recycled with glass fibre (GF) reinforcement to develop a unique remediate material. Therefore, this study fabricated (1) a glass fibre-carbon prepreg waste reinforced polymer hybrid composite (GF-CPW-PP), (2) a polypropylene composite (PP), (3) a carbon prepreg waste reinforced composite (CPW-PP), and (4) a glass fibre reinforced composite (GF-PP) and reported their degradation and residual tension properties after immersion in water. The polymer hybrid composites were fabricated via extrusion technique with minimum reinforce glass-carbon prepreg waste content of 10 wt%. The immersion test was conducted at room temperature using distilled water. Moisture content and diffusion coefficient (DC) were determined based on water adsorption values recorded at 24-h intervals over a one-week period. The results indicated that GF-PP reinforced composites retained the most moisture post-168 h of immersion. However, hardness and tensile strength were found to decrease with increased water adsorption. Tensile strength was found to be compromised since pores produced during hydrolysis reduced interfacial bonding between glass fibre and prepreg carbon reinforcements and the PP matrix.

Keywords: hybrid composites; carbon prepreg waste; water absorption; degradation

1. Introduction

Carbon fibre (CF) is a high-strength synthetic fibre with a micro graphite crystal structure. It is mainly used as a filler or fibre reinforcement to strengthen composite materials [1–5] since it is not only lightweight but possesses the highest specific modulus and highest specific strength in comparison to other fibre reinforcements. General and high-technology industries utilise CF due to these excellent properties. In the high-technology industry, the aerospace sector, as well as the nuclear engineering sector, use it to manufacture components, such as the Boeing 787 Dreamliner and Airbus A350. The general and transportation industries, however, use CF to produce components such as fan blades, bearings, and gears, among other things. The aerospace industry relies the heaviest on CF since about

50% of an airplanes' body is made of it. A study by General Motors Research & Development Center concluded that studying various advanced CF fabrication methods was the best way to optimise its properties. The demand for CF in the aerospace, industrial and sport equipment sectors is estimated to expand by a 1:1 ratio [6].

As of 2019, the global demand for CF is approximately 100,000 metric tons with an annual growth rate of 10% to 12% in comparison to 85,000 metric tons in 2018. This annual growth rate is estimated to increase by approximately 7.6% per year by 2024 [7]. This will inevitably increase the amount of CF waste to be managed with minimal environmental impact. Moreover, in a bid to encourage compliance with waste treatment policies and promote recycling, the European Union (EU) has introduced numerous legislative measures to limit waste disposal methods such as landfills and incineration. However, CF composites are particularly hard to recycle due to the cross-linked thermoset polymers in their matrices. Furthermore, other reinforcements are usually incorporated in its base constituents, thus creating complex multiphase waste [8]. This means that even if CF waste can be recycled, it would be hard to preserve its original properties.

Numerous studies have explored CF waste management options. A study by Gopalraj and Kärki [9] evaluated existing CF waste-glass fibre (GF) reinforced composites recycling and also fibre recovery methods and determined the properties retained before identifying gaps in the material's lifecycle within a circular economy. Yang et al. examined the chemicals used to recycle CF and GF epoxy resin composites; polyethylene glycol (PEG) and sodium hydroxide (NaOH). Their study concluded that recycled CF and non-alkaline GF retain 94% to 96% of their original strength and that recycled medium-alkali GF retained less than 90% of its tensile strength [10]. Tomioka et al. fabricated carbon prepreg waste (CPW) reinforced composites via injection moulding and studied the palletisation process. With respect to mechanical and flowability properties, they found that recycled CF had greater impregnation in the composites due to finer interfacial adhesion compared to virgin conventional materials [11].

There are different interpretations of conditions that cause CF and GF degradation. It is thought to occur when the materials are exposed to or absorb moisture with a few studies verifying this assumption. Cauich-Cupul et al. discovered that moisture uptake in CF/epoxy matrix composites correlated to a decrease of its glass transition temperature and deteriorated the interfacial shear properties [12]. An analysis by Eslami et al. showed that GF composites exposed to humid conditions in an aging environment changed from seawater to water causing a decrease in the failure force (from 35.1% to 51.8% kN) and reducing maximum displacement (from 26.2% to 31.6%) as the aging temperature rose from 2 °C to 25 °C [13]. Tsai et al. [14] investigated CF/GF hybrid composites. The CF/GF composites appeared to be more complex under these conditions. Short beam shear strength and glass transition temperature appeared to retain 77% and 98%, respectively, of their respective properties. This was attributed to the high density packing of CF/GF fibre interfaces which allowed only moderate damage to fibre-matrix interface.

The literature review reveals the many drawbacks of CF composites such as degradation of properties after the expiry date as well as the high manufacturing cost. The degradation of CPW is, especially, uncertain and has not been investigated further. The first issue arises when the CPW material passes its expiry date once the matrix has cured. This causes it to harden and become inflexible and unreliable despite its usually exemplary mechanical properties. As more and more CP is used, it will produce an exorbitant amount of CP waste. As we are surrounded by moisture, the behaviour of CPW after water degradation warrants examination as such an investigation can be beneficial to both local and global advancement of the material.

In this study, a glass fibre-carbon prepreg waste reinforced polymer hybrid composite (GF-CPW-PP), a polypropylene composite (PP), a carbon prepreg waste reinforced composite (CPW-PP), and a glass fibre reinforced composite (GF-PP) were immersed in distilled water at room temperature to investigate the effects of moisture. The moisture absorption behaviour of these specimens was

then evaluated. Since the specimens were in tensile form, their tensile properties prior to and after immersion were analysed as well.

2. Materials and Methods

2.1. Materials

For the purposes of this study, four composites were made of polypropylene (PP) matrix only, PP reinforced with carbon prepreg waste (CPW), PP reinforced with glass fibre (GF), and PP reinforced with both GF and CPW. The CPW used was a twill weave carbon fibre fabric pre-impregnated with an epoxy resin system of 0.3 mm thickness and 1.21×10^{-6} kg/c mm^3 density from Fibre Glast Developments Corporation, Ohio, USA While the GF reinforcement was a 450 g/m^2 E-type chopped strand mat (CSM). The PP (CAS #: 9003-07-0) provided by LOTTE CHEMICAL TITAN Holding Berhad, Malaysia, was the TITANPRO® 6331 grade with a molecular weight of 354.57 kg/mol, melt mass flow rate (230 °C/2.16 kg) of 14 g/10 min, density of 0.9 g/cm^3 and tensile strength at yield of 35.3 MPa.

2.2. Preparations of Hybrid Composites

The composites were prepared via extrusion. The GF and CPW were first ground using the FRITSCH Cross Beater Mill PULVERISETTE 16 and the 0.75 mm cast iron grinding insert. The ground GF was ~10 μm while the ground CPW was ~5 μm. Different variations of GF and CPW were then mixed with PP using the 27 mm-diameter screw of a Leistritz Advanced Technologies Corporation MICRO 27 GL-32D extruder machine to form two reinforced composites (GF-PP and CPW-PP), one composite (PP), and one hybrid composite (GF-CPW-PP). The composites were extruded in a length to diameter (L/D) ratio of 32D at 180 °C and pressure of 66.9 bar. The twin-screw extruder speed was 10 rpm and the flow rate was 1.7 g/min. The four specimens were labelled (1) PP and contained 100 wt% polypropylene, (2) GF-CPW-PP and contained 5 wt% glass fibre and 5 wt% carbon prepreg waste, (3) CPW-PP and contained 10 wt% carbon prepreg waste, and (4) GF-PP and contained 10 wt% of glass fibre, as shown in Figure 1.

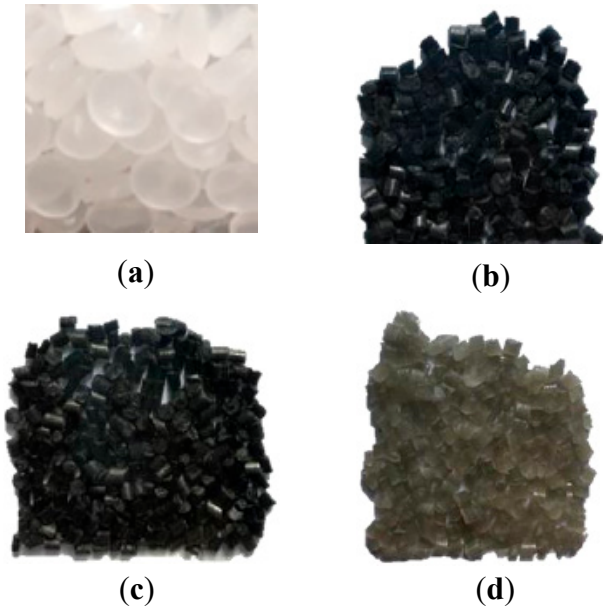

Figure 1. Extruded composites (**a**) polypropylene composite (PP); (**b**) glass fibre-carbon prepreg waste reinforced polymer hybrid composite (GF-CPW-PP); (**c**) CPW-PP; and (**d**) GF-PP.

2.3. Material Characterization

2.3.1. Water Immersion Tests

Water uptake was measured by repeatedly immersing the specimens in distilled water at room temperature then measuring the weight in accordance with the Standard Test Method for Moisture Absorption Properties and Equilibrium Conditioning of Polymer Matrix Composite Materials (ASTM D5229). Prior to immersion, the tensile properties were determined in accordance with the Standard Test Method for Tensile Properties of Polymer Matrix Composite Materials (ASTM D3039). Throughout the immersion process, the specimen weights were measured at 24 h, 48 h, 72 h, 96 h, 120 h, 144 h, and 168 h. The weight percentage during the immersion test was measured as follows,

$$\boldsymbol{W_P}, \% = \frac{\boldsymbol{W_1 - W_0}}{\boldsymbol{W_0}} \times \mathbf{100} \quad (1)$$

where W_P,% is the weight percentage of moisture content, W_1 is the post-immersion weight, and W_0 is the pre-immersion weight.

2.3.2. Tensile Test

The tensile test was performed according to ASTM D3039 standards at room temperature with 1.0 mm/min crosshead speed and 10 kN load cell. Rectangular specimens measuring 250 mm × 25 mm × 2.5 mm (length × width × thickness) were tested. The tensile properties of the specimens pre- and post-168 h of immersion were compared.

2.3.3. Hardness Test

The Rockwell hardness testing method was used to measure the impression depths on the specimens' surfaces under applied loads. It was conducted in accordance with ASTM D785 standards and measured in Rockwell (R) scales. A piece of a specimen was cut then placed on the surface tester at zero gauge before a minor load was applied. A major load was then applied for 4 s then shifted back to the minor load before the hardness value was recorded.

2.3.4. Morphology

Scanning Electron Microscopy (SEM) is a test method that produces magnified images for analysis under an electron beam. This method is used to obtain images of a material's surface and texture, especially for failure analysis. The images are in high resolution and able to precisely measure minute features on an object at high magnifications. The specimens were cut into approximately 1 cm × 1 cm pieces and clipped into the sample holders. They were then loaded into the equipment and analysed by adjusting the magnification and focus.

3. Results and Discussion

3.1. Water Immersion

Since the appearance of a specimen's surface is likely to affect its application, the goal was to innovate various aspects of it with or without changing its condition. For any given material, water immersion affects its characteristics based to the material's content, structural arrangement of its individual elements, fabrication method, etc. [15–20]. A visual assessment showed that specimens immersed in distilled water varied in colour (Figure 2). PP was white while GF was grey and CPW was black. However, the GF-CPW-PP specimen initially appeared charcoal but eventually turned black as the carbon emerged allowing less light to be reflected giving it a close to zero albedo in the perceivable spectrum region. Specimen discoloration after prolonged exposure was observed. The composites changed from their original colour to a faded colour due to modifications in the matrix. As reported, the colours change in reaction to the functional group adhering to the carbon polymer chain [21].

Furthermore, morphological changes in specimen surfaces were observed post-immersion as well. While the PP specimen was slightly smooth and did not differ greatly to its surface morphology prior to immersion, the reinforced composite specimens had rougher surfaces due to fractional debonding as seen in the CPW-PP and GF-PP specimens.

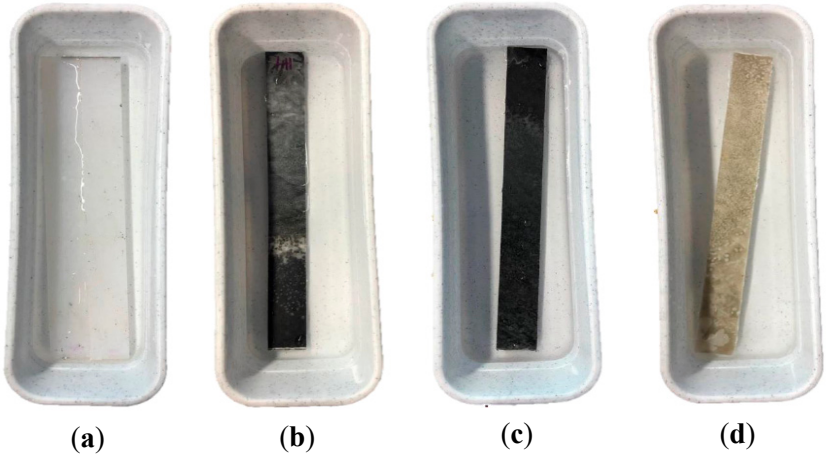

Figure 2. Specimens immersed in distilled water (**a**) PP (**b**) GF-CPW-PP; (**c**) CPW-PP; and (**d**) GF-PP.

The moisture content of the PP and other composites (GF-CPW-PP, CPW-PP, and GF-PP) immersed in distilled water for 168 h are shown in Figure 3. While similar trends emerged, the difference in values may be due to dissimilarities in the specimens' percentage of moisture as a function of square root time. The moisture content percentage value was found to increase with immersion time. This trend increased sharply indicating accelerated moisture penetration due to active moisture penetrability and capillary action. GF-PP had the highest moisture content percentage (4.7%) followed by GF-CPW-PP (3.4%), CPW-PP (3.2%), and finally PP (0.5%). The covalent bonds between the GF-PP specimen's walls enabled more water molecules to be absorbed. Therefore, the addition of GF in GF-CPW-PP weakened interfacial forces and increased the surface tension.

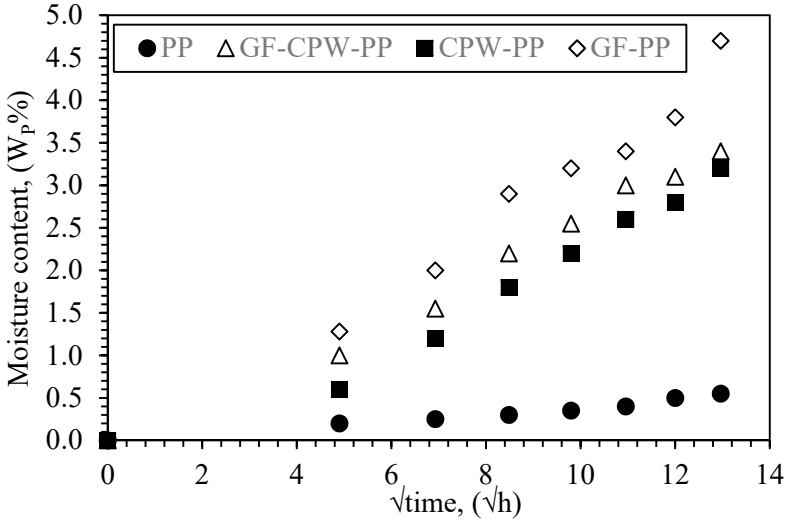

Figure 3. Water content percentage (%) of specimens in distilled water condition.

The moisture absorption properties analysis of the immersed specimens was completed by quantifying the diffusion coefficient (D_C). The D_C value of the specimens was calculated using Equation (2) [22].

$$D_C = \pi \left(\frac{kh}{4\, M_m} \right)^2 \quad (2)$$

where k is the initial slope from the curve in W_P (%) versus √time (√h) figure, h is the thickness of the specimen (mm) and M_m (%) is the maximum weight gained (%). As seen in Table 1, GF-CPW-PP had the highest D_C value followed by GF-PP and CPW-PP. This could be caused by the hydrolysis mechanism of CPW and GF.

Table 1. Value of diffusion coefficient, D_C and the maximum moisture content, M_m.

	Unit	PP	GF-CPW-PP	CPW-PP	GF-PP
Diffusion Coefficient, D_C, $\times 10^{-3}$	mm^2/s	4.0	4.6	3.9	3.8
Maximum Moisture Content, M_m	%	0.5	3.4	3.2	4.7

The hydrolysis of the composites was noticeable in distilled water. The expected mechanisms of composites GF-CPW-PP, CPW-PP, and GF-PP in distilled water are illustrated in Figure 4. In distilled water, it is possible that the electronegative ions of the liquid had an active hold on the diffusion mechanism. This allowed the CPW, GF and PP to swell and explains the excess of positive charges surrounding them. The excess of positive charges triggered the COO^- and OH^- chemical bonds in CPW. With regard to electronegative charges, GF-CPW-PP had the highest value followed by CPW-PP and GF-PP. This correlated with the results of previous studies by Oliveux et al. [23] and Uthaman et al. [24]. The presence of H+ ions in the liquid is typically regarded as a catalyst and thought to highly influence the degradability of hybrid composites.

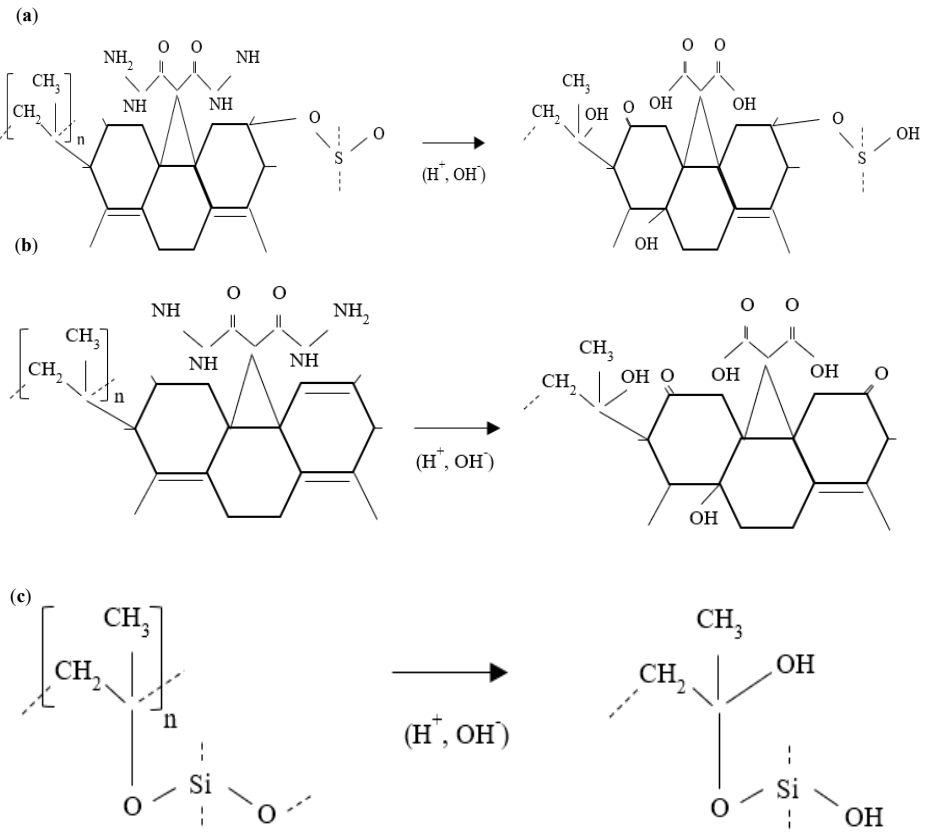

Figure 4. Scheme proposed of hydrolysis mechanism for (**a**) GF-CPW-PP, (**b**) CPW-PP and (**c**) GF-PP.

It has been previously exhibited that the diffusional permeability of H_2O particles into hybrid composites is possibly caused by sorption. Therefore, the verification of sorption coefficient (S_P) is regularly used to estimate the diffusional permeability of H_2O into hybrid composites. In this work, the sorption coefficient (S_P) is defined in Equation (3),

$$S_P = \frac{M_S}{M_C} \tag{3}$$

where M_S is the weight gained by the specimen in equilibrium and M_C is the mass of the specimen. Meanwhile, the permeability coefficient (P_P) would show the S_P and D_C and can be verified using Equation (4).

$$P_P = S_P \,.\, D_C \tag{4}$$

The S_P and P_P values of the immersed composites are shown in Table 2. GF-PP had the highest P_P value followed by GF-CPW-PP and CPW-PP. The cause for this different range of action in the composites is mainly accredited to the appearance of radial interfaces in GF and CPW. Cracks were seen to enlarge due to weight gain and distilled water infiltration. Therefore, this investigation successfully simulated the moisture absorption mechanism of the composites.

Table 2. Value of sorption coefficient, S_P and the permeation coefficient P_C of specimen immersed in distilled water.

	Unit	PP	GF-CPW-PP	CPW-PP	GF-PP
Sorption Coefficient, S_P	g/g	0.0785	0.4478	0.4075	0.5985
Permeability Coefficient, *Pc*	mm^2/s	0.0003	0.0021	0.0016	0.0023

3.2. Tensile Test

The PP composite, both reinforced composites (CPW-PP and GF-PP), and the hybrid composite (GF-CPW-PP) were immersed in distilled water for a total of 168 h prior to tensile loading to examine their mechanical properties. All specimens demonstrated extreme failure under the maximum load indicating a stress-strain correlation commonly detected in brittle fractures (Figure 5). Although the composites initially had random inclusion of the fibre reinforcements, tensile micro cracks began to grow on the weakest plane close to the fibre reinforcement notch tip during tensile loading. The weakest plane was affected by water molecule ingress through micro cracks and the edges of the fibre-matrix structure [25–27]. Over time, degradation weakened the stress transfer mechanism and caused debonding. The micro cracks in the specimens later formed large fracture scale linkage and failed without necking.

As previously mentioned, increased moisture in the specimens led to degradation and impacted mechanical performance. Water ingress influenced crack propagation and accelerated the failure mechanisms weakening the performance of, otherwise, well-built structures. Figure 6 shows the stress-strain curves of immersed specimens vs. control specimens (not immersed) in the tensile strength test. The tensile strength all the composites decreased after 168 h of immersion in distilled water. Table 3 clearly shows the difference between the specimens, where GF-CPW-PP had the highest tensile strength (78.5 ± 2.3 MPa) followed by CPW-PP and GF-PP with 73.2 ± 5.8 MPa and 69.5 ± 2.1 MPa, respectively. Therefore, the tensile strength of immersed composites decreased as a consequence of moisture absorption.

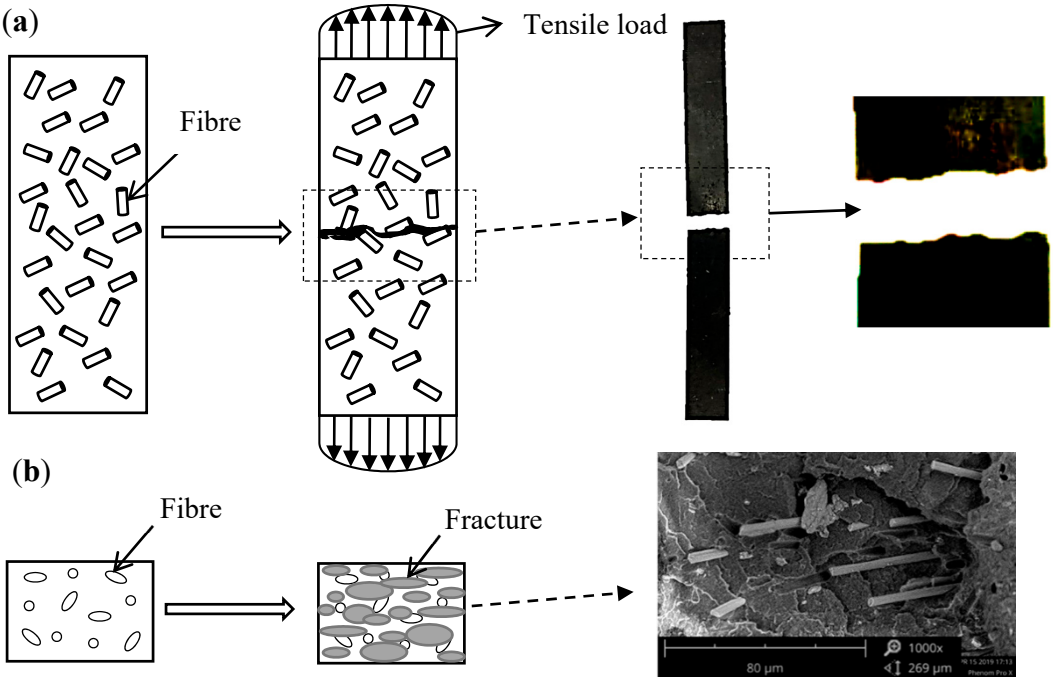

Figure 5. Fracture condition of specimen immersed in distilled water (**a**) side view; and (**b**) top view.

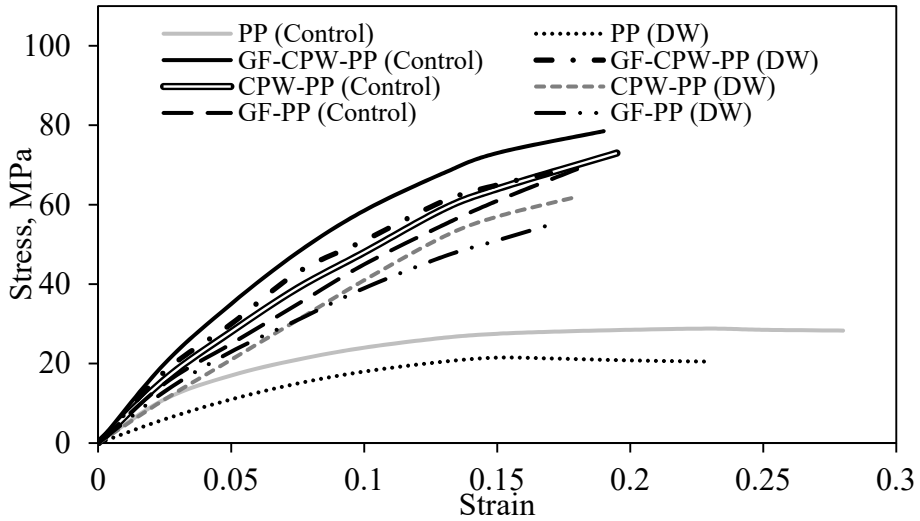

Figure 6. Stress-strain curves of specimens in control and immersed condition.

Table 3. Value of tensile strength, elastic modulus and elongation at break for control specimens and immersed in distilled water condition.

		Tensile Strength (MPa)	Elastic Modulus (MPa)	Elongation at Break (%)
PP	**Control**	28.8 ± 1.4	203.8 ± 8.1	28.0 ± 3.1
	DW	21.5 ± 1.0	157.7 ± 6.3	23.0 ± 2.5
GF-CPW-PP	**Control**	78.5 ± 2.3	640.0 ± 51.2	19.0 ± 2.1
	DW	69.3 ± 2.0	573.3 ± 45.9	18.7 ± 1.7
CPW-PP	**Control**	73.2 ± 5.8	520.0 ± 36.4	19.5 ± 1.8
	DW	62.7 ± 5.1	420.0 ± 29.4	17.5 ± 1.4
GF-PP	**Control**	69.5 ± 2.1	466.6 ± 32.6	18.0 ± 1.1
	DW	55.1 ± 1.6	413.3 ± 28.9	17.2 ± 1.0

3.3. Hardness Test

Hardness measurement, in general, depends on the selected application and deliberated material. Although common quantification methods are used, minor dissimilarity; such as stiffness variability; occur during measurement. The hardness values, according to the Rockwell (HRR) scale, based on the structural indentation of the specimens is shown in Figure 7. Prior to immersion, GF-CPW-PP had the highest HRR value (103) followed by PCW-PP, GF-PP, and PP with 99, 93, and 89, respectively. Post-168 h of immersion, the hardness test was performed again. The immersed specimens showed a decreasing trend in hardness. GF-CPW-PP, once again, had the highest HRR value (98) followed by CPW-PP, GF-PP, and PP with 93, 86, and 80, respectively.

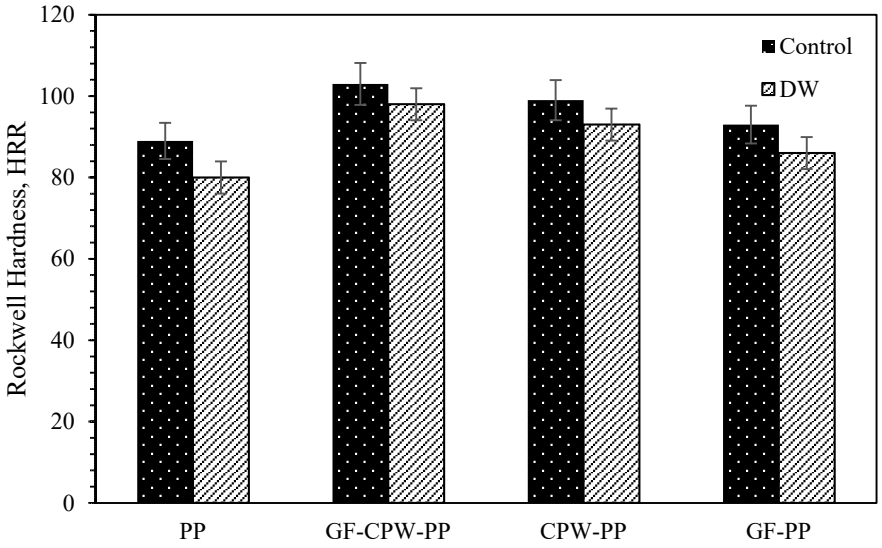

Figure 7. Hardness of the control and immersed specimens.

The change in hardness were a function of moisture absorption. The correlation between hardness and sorption coefficient is shown in Figure 8. This may have caused the densification of the specimens and possibly the pores within the interfacial bond between fibres and matrix as depicted by the SEM micrograph. Despite the addition of fibre reinforcement, composites demonstrated decrease in hardness as expected by the transformation of the sheared GF and/or CPW to deform the fibres around the PP. This caused a large non-agglomeration from decomposition of the integrated fibres [28,29] leading to increased internal porosity and further decrease in hardness. Other than that, the incorporation of 10% fibre reinforcement led to minor differences in hardness value. Therefore, although the addition of fibre reinforcement increased the rigidity of the composites, it caused porosity and a less integrate fibre structure that decreased hardness.

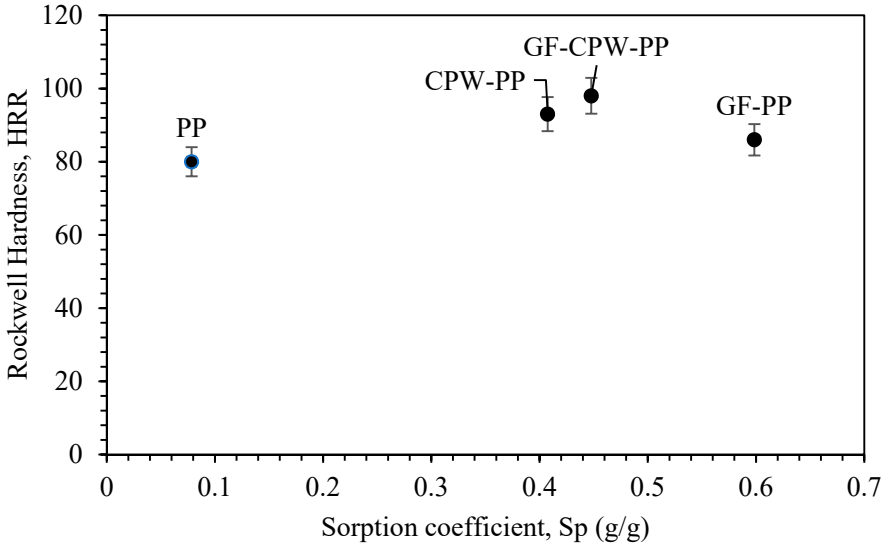

Figure 8. Effect of the hardness on the sorption coefficient of the specimens.

3.4. Morphology

The morphology of control and immersed specimens (GF-CPW-PP, CPW-PP and GF-PP) was observed. The radical parts of the composites formed brittle fractures, whereas the obscured parts were the moisture. As the D_C of the obscured part increased at a particular rate, depending on the type of the fibre reinforcement and the fabrication techniques, reinforcement fractures persisted. It was observed that GF had the highest moisture aspect which correlated to its moisture content percentage. Therefore, GF-PP was expected to allow moisture to occupy the region. Figure 9 shows the internal fractures in the control and immersed CPW-GF-PP, CPW-PP and GF-PP specimens after extensible testing. It was observed that PCW was dark while GF was white. The GF and CF in the composites were ~8 µm and ~3 µm, respectively, with clearly observable textures. The surface texture of the specimens was not smooth. GF and CPW seemed randomly oriented and were easily observable in micrographs of the interior as the interfacial adhesion between the fibres and the PP matrix were weak. Greater distilled water dispersion in the PP matrix was seen in composites containing GF. GF-PP disintegrated as moisture penetrated deep into its interfacial adhesion. However, GF-PP had the lowest GF content in comparison to CPW-PP and GF-CPW-PP. Previous studies reported that [30–33] composite failure mechanisms may be represented as follows: when there is no load disruption by the reinforcement break under mechanical testing, the load is uniformly distributed among the fibres next to the break fibre resulting in a degree of concentrated stress developing on those fibres and damaging the surrounding matrix. Therefore, the presence of intense moisture increased vulnerability and decreased the tensile strength of the composites.

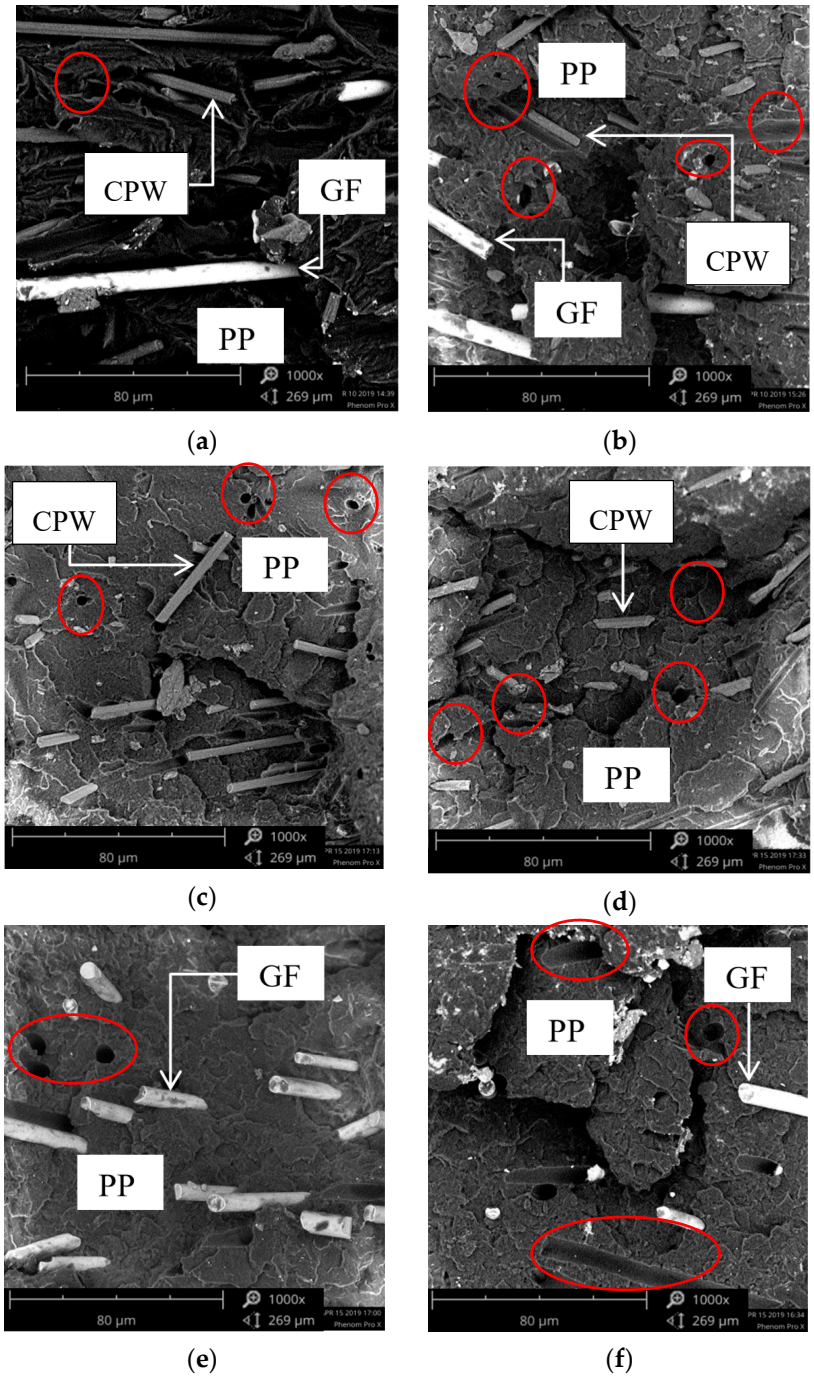

Figure 9. SEM images of (**a**) GF-CPW-PP (control); (**b**) GF-CPW-PP (DW); (**c**) CPW-PP (control); (**d**) CPW-PP (DW); (**e**) GF-PP (control), and (**f**) GF-PP (DW) specimens. (red circle shows porosity).

4. Conclusions

In this study, the immersion test of the composites showed increasing moisture content over time. The maximum moisture content obtained was in the following order: GF-PP > GF-CPW-PP > CPW-PP > PP. The tensile strength for all immersed specimens decreased in comparison to control specimens (not immersed). The tensile strengths, in descending order, were: GF-CPW-PP > CPW-PP > GF-PP > PP. In comparison to pure PP, the tensile strength of GF-CPW-PP was found to have increased by 272.6% and by 254.1% in CPW-PP and by 241.3% in GF-PP. However, the hardness of all specimens showed a decreasing trend. The Rockwell (HRR) values of GF-CPW-PP decreased from 103 to 98,

from 99 to 93 in CPW-PP, from 93 to 86 in GF-PP, and from 89 to 80 in PP. This indicated that moisture absorbed by the specimens caused decreased interfacial bonding between fibre reinforcements and the PP matrix, thereby causing the composites to disintegrate.

Author Contributions: Conceptualization, N.N.; methodology, M.R.Z., W.F.F.W.A., N.N. and M.I.; formal analysis, N.N.; investigation, F.J., N.N.; resources, H.F.A.M. and N.N.; data curation, N.N. and H.F.A.M.; writing—original draft preparation, N.N.; writing—review and editing, N.N.; visualization, N.N.; supervision, N.N.; project administration, N.N.; funding acquisition, N.N. All authors have read and agreed to the published version of the manuscript.

Funding: This research was funded by Fundamental Research Grant Scheme grant number FRGS/1/2019/TK05/UTP/03/2.

Acknowledgments: The authors wish to thank the Ministry of Education Malaysia for their financial support through Fundamental Research Grant Scheme (FRGS/1/2019/TK05/UTP/03/2).

Conflicts of Interest: The authors declare no conflict of interest.

References

1. Chand, S. Review: Carbon fiber composites. *J. Mater. Sci.* **2000**, *35*, 1303–1313. [CrossRef]
2. Taketa, I.; Kalinka, G.; Gorbatikh, L.; Lomov, S.V.; Verpoest, I. Influence of cooling rate on the properties of carbon fiber unidirectional composites with polypropylene, polyamide 6, and polyphenylene sulfide matrices. *Adv. Compos. Mater.* **2020**, *29*, 101–113. [CrossRef]
3. Miao, C.; Hareesh, V.T. Effect of Loading Rate on Fracture Behavior of Carbon Fiber Reinforced Polymer Composites. In *Challenges in Mechanics of Time Dependent Materials, Fracture, Fatigue, Failure and Damage Evolution*; Springer: Berlin/Heidelberg, Germany, 2020; Volume 2, pp. 21–28.
4. Capela, C.; Oliveira, S.E.; Ferreira, J.A. Fatigue behavior of short carbon fiber reinforced epoxy composites. *Compos. Part. B Eng.* **2019**, *164*, 191–197. [CrossRef]
5. Xu, P.; Yu, Y.; Liu, D.; He, M.; Li, G.; Yang, X. Enhanced interfacial and mechanical properties of high-modulus carbon fiber composites: Establishing modulus intermediate layer between fiber and matrix based on tailored-modulus epoxy. *Compos. Sci. Technol.* **2018**, *163*, 26–33. [CrossRef]
6. Huang, X. Fabrication and properties of carbon fibers. *Materials* **2009**, *2*, 2369–2403. [CrossRef]
7. Pichler, D.; Mazumdar, S.; Benevento, M.; Seneviratine, W.; Liang, R.; Witten, E. The Carbon Fiber Market, Composites Manufacturing: 2020 State of the Industry Report, January–February Issue, 2020. Available online: http://compositesmanufacturingmagazine.com/2020/01/2020-state-of-the-industry-report/2/ (accessed on 3 January 2020).
8. Witik, R.; Teuscher, R.; Michaud, V.; Ludwig, C.; Månson, J. Carbon fibre reinforced composite waste: An environmental assessment of recycling, energy recovery and landfilling. *Compos. Part A Appl. Sci. Manuf.* **2013**, *49*, 89–99. [CrossRef]
9. Gopalraj, S.K.; Kärki, T. A review on the recycling of waste arbon fibre/glass fibre-reinforced composites: Fibre recovery, properties and life-cycle analysis. *SN Appl. Sci.* **2020**, *2*. [CrossRef]
10. Yang, P.; Zhou, Q.; Li, X.Y.; Yang, K.K.; Wang, Y.Z. Chemical recycling of fiber-reinforced epoxy resin using a polyethylene glycol/NaOH system. *J. Reinf. Plast. Compos.* **2014**, *33*, 2106–2114. [CrossRef]
11. Tomioka, M.; Ishikawa, T.; Okuyama, K.; Tanaka, T. Recycling of carbon-fiber-reinforced polypropylene prepreg waste based on palletization process. *J. Compos. Mater.* **2017**, *51*, 3847–3858. [CrossRef]
12. Cauich-Cupul, J.I.; Perez-Pacheco, E.; Valadez-Gonzalez, A.; Herrera-Franco, P.J. Effect of moisture absorption on the micromechanical behavior of carbon fiber/epoxy matrix composites. *J. Mater. Sci.* **2013**, *48*, 1873–1882. [CrossRef]
13. Eslami, S.; Hanorbakhsh-Raouf, A.; Eslami, S. Effects of moisture absorption on degradation of E-glass fiber reinforced Vinyl Ester composite pipes and modelling of transient moisture diffusion using finite element analysis. *Corros. Sci.* **2015**, *90*, 168–175. [CrossRef]
14. Tsai, Y.I.; Bosze, E.J.; Barjasteh, E.; Nutt, S.R. Influence of hygrothermal environment on thermal and mechanical properties of carbon fiber/fiberglass hybrid composites. *Compos. Sci. Technol.* **2009**, *69*, 432–437. [CrossRef]
15. Mahdi, A.S.; Mohsin, N.R. Water absorption and fatigue life of an Epoxy composite reinforced by glass fiber. In *IOP Conference Series: Materials Science and Engineering*; IOP Publishing: Bristol, UK, 2018; Volume 454.

16. Wang, L.; Wang, M.; Guo, M.; Ye, X.; Ding, T.; Liu, D. Numerical Simulation of Water Absorption and Swelling in Dehulled Barley Grains during Canned Porridge Cooking. *Processes* **2018**, *6*, 230–243. [CrossRef]
17. Shiyuan, H.; Junjie, W.; Zhenfeng, Q.; Kai, K. Effects of cyclic wetting-drying conditions on elastic modulus and compressive strength of sandstone and mudstone. *Processes* **2018**, *6*, 234–250.
18. Espert, A.; Francisco, V.; Sigbritt, K. Comparison of water absorption in natural cellulosic fibres from wood and one-year crops in polypropylene composites and its influence on their mechanical properties. *Compos. Part A Appl. Sci. Manuf.* **2004**, *35*, 1267–1276. [CrossRef]
19. Mohebby, B.; Younesi, H.; Ghotbifar, A.; Kazemi-Najafi, S. Water and moisture absorption and thickness swelling behavior in polypropylene/wood flour/glass fiber hybrid composites. *J. Reinf. Plast. Compos.* **2009**, *29*, 830–839. [CrossRef]
20. Tuncdemir, A.R.; Aykent, F. Effect of fibers on the color change and stability of resin composites after accelerated aging. *Dent. Mater. J.* **2012**, *31*, 872–878. [CrossRef]
21. Dhakal, H.N.; MacMullen, J.; Zhang, Z. Chapter 5: Moisture measurement and effects on the properties of marine composites. In *Marine Applications of Advanced Fibre-Reinforced Composites*; Woodhead Publishing: Cambridge, UK, 2015; pp. 103–122.
22. Oliveux, G.; Bailleul, J.L.; La Salle, E.L.G.; Lefèvre, N.; Biotteau, G. Recycling of glass fibre reinforced composites using subcritical hydrolysis: Reaction mechanisms and kinetics, influence of the chemical structure of the resin. *Polym. Degrad. Stab.* **2013**, *98*, 785–800. [CrossRef]
23. Uthman, A.; Xian, G.; Thomas, S.; Wang, Y.; Zheng, Q.; Liu, X. Durability of an epoxy resin and its carbon fiber-reinforced polymer composite upon immersion in water, acidic, and alkaline solutions. *Polymer* **2020**, *12*, 614–637. [CrossRef] [PubMed]
24. Masuelli, M.A. Chapter 1: Introduction of Fibre-Reinforced Polymers—Polymers and Composites: Concepts, Properties and Processes. In *Fiber Reinforced Polymers—The Technology Applied for Concrete Repair*; INTECH Open Access Publisher: Rijeka, Croatia, 2013.
25. Colquhoun, R.; Tanner, K.E. Mechanical behaviour of degradable phosphate glass fibres and composites—A review. *Biomed. Mater.* **2016**, *11*, 014105. [CrossRef]
26. Sethi, S.; Ray, B.C. Fibre/Polymer Interface Integrity on Structural Strength and Stability. *Microscopy* **2019**.
27. Available online: https://analyticalscience.wiley.com/do/10.1002/micro.2983/full/ (accessed on 18 September 2019).
28. Zainal, Z.; Ismail, H. Polypropylene/(waste tire dust)/(short glass fiber composites): Effects of silane coupling agent and dynamic vulcanization. *J. Vinyl Addit. Technol.* **2011**, *17*, 245–253.
29. Babu, R.R.; Naskar, K. Recent developments on thermoplastic elastomers by dynamic vulcanization. In *Advanced Rubber Composites*; Springer: Berlin/Heidelberg, Germany, 2010; pp. 219–247.
30. Yamamoto, G.; Koizumi, K.; Okabe, T. Tensile Strength of Unidirectional Carbon Fiber-Reinforced Plastic Composites. In *Strength of Materials*; IntechOpen: London, UK, 2019.
31. Okabe, T.; Takeda, N. Size effect on tensile strength of unidirectional CFRP composites—Experiment and simulation. *Compos. Sci. Technol.* **2002**, *62*, 2053–2064. [CrossRef]
32. Vanegas-Jaramillo, J.D.; Patiño-Arcila, I.D. Fragmentation model for the tensile response of unidirectional composites based on the critical number of fiber breaks and the correction of the fiber-matrix interfacial strength. *Lat. Am. J. Solids Struct.* **2019**, *16*. [CrossRef]
33. Truong, G.T.; Tran, H.V.; Choi, K.K. Tensile Behavior of Carbon Fiber-Reinforced Polymer Composites Incorporating Nanomaterials after Exposure to Elevated Temperature. *J. Nanomater.* **2019**, *2019*, 1–14. [CrossRef]